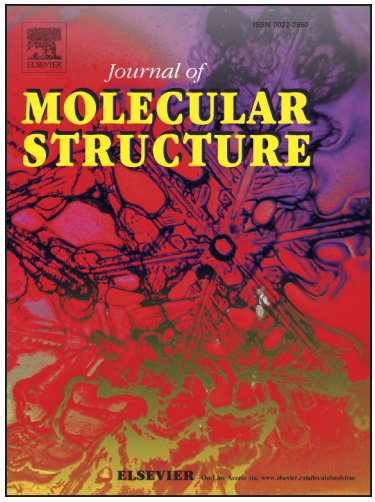

Synthesis and spectroscopic characterization of a new (aryl-SCN)$_n$ polymer: Polythiocyanatohydroquinone

Gleb V. Baryshnikov, Rostislav L. Galagan, Ludmila P. Shepetun, Valentina A. Litvin, Boris F. Minaev

PII: S0022-2860(15)00383-X
DOI: http://dx.doi.org/10.1016/j.molstruc.2015.04.040
Reference: MOLSTR 21494

To appear in: *Journal of Molecular Structure*

Received Date: 3 February 2015
Revised Date: 25 April 2015
Accepted Date: 28 April 2015

Please cite this article as: G.V. Baryshnikov, R.L. Galagan, L.P. Shepetun, V.A. Litvin, B.F. Minaev, Synthesis and spectroscopic characterization of a new (aryl-SCN)$_n$ polymer: Polythiocyanatohydroquinone, *Journal of Molecular Structure* (2015), doi: http://dx.doi.org/10.1016/j.molstruc.2015.04.040

Synthesis and spectroscopic characterization of a new (aryl-SCN)$_n$ polymer: polythiocyanatohydroquinone

Gleb V. Baryshnikov,* Rostislav L. Galagan, Ludmila P. Shepetun, Valentina A. Litvin, Boris F. Minaev

Department of Organic Chemistry,
Bohdan Khmelnytsky National University, 18031 Cherkasy, Ukraine

* Corresponding author. Tel.: +38 0472 376576; fax: +38 0472 354463.
E-mail address: glebchem@rambler.ru, bfmin@rambler.ru (Gleb V. Baryshnikov)

Abstract

In the present work we have demonstrated the first synthesis of the polythiocyanogen-like (aryl-SCN)$_n$ compound (polythiocyanatohydroquinone) from the initial 1,4-benzoquinone and NH_4SCN reagents under the normal conditions in the glacial acetic acid medium. The synthesized amorphous polymer was characterized experimentally by the FT-IR and UV-vis spectroscopic methods accompanied with theoretical assignments by the density functional theory (DFT) and time-dependent DFT calculations. The transmission electron microscopy and the XRD pattern analysis were used to indicate the amorphous structure of the synthesized polymer. The DFT geometry optimization of a number of oligomers (n=4-8) permit us to predict the possible structure of polythiocyanatohydroquinone and to assign the observed bands in IR and UV-vis absorption spectra

It was found that the synthesized polythiocyanatohydroquinone powder has a complicated structure which can be represented as a branched polymer constructed from the mono- and doubly- SCN-substituted benzene-1,4-diol moieties. This new material demonstrates a good stabilizing effect in respect to colloidal solutions of Ag and Au nanoparticles. Additionally, polythiocyanatohydroquinone is predicted to be a promising candidate for creation of metal-containing composite materials. Its application as a framework for the Pt electrode closing is found very useful.

Keywords: polythiocyanatohydroquinone, FT-IR spectra, UV-vis spectra, DFT calculations, electronic transition, branched polymer.

1. Introduction

During last decades the organic polymers attract the growing interest because of their wide applications in molecular electronics and power sources technologies. [1–9] Such polymers can be applied as the charged-carriers transfer layers in organic light-emitting diodes (OLEDs), in plastic solar cells, or as photo- and electroluminescence generation materials in various power-conversion devices [1–4]. It is especially valuable if the one and the same monomer has a tendency toward production of polymers which differ in a number of the growth dimensions (i.e. 1D linear chains, 2D frameworks and 3D superstructures) [5–7]. For example, the tetraphenylporphyrin, phthalocyanine and tetraoxa[8]circulene can form the linear 1D and reticular 2D polymers greatly differ in their semiconducting properties [5, 8–10]. There are many other examples of such bifunctional monomers [5] and one of them is the inorganic thiocyanogen monomer $(SCN)_2$ [11] which can be obtained by oxidation of the SCN^- anion. Free thiocyanogen is an unstable compound which polymerizes quickly producing the insoluble polythiocyanogen $(SCN)_n$ [11]. This polymer is known for a long time and some ways for its practical utilization were proposed including the photocatalytic applications [12–14] and photovoltaic [15–17] devices. However, there is no consensus in the literature concerning the structure of the $(SCN)_n$ polymer. The most reliable structure of $(SCN)_x$ in the form of 1,2,4-dithiazole rings linked by nitrogen bridges (Fig. 1, a) was proposed recently by Woollins and coauthors [18] on the ground of the NMR, IR, and Raman spectral data of high quality which were accompanied by the MALDI TOF mass-spectroscopic data. From the other hand, Cataldo et. al. have proposed the rather different $(SCN)_x$ structures in the form of linear unbranched $–(S–C=N)_x–$ chains [19] or in the form of $–(C=N)_x–$ chains cross-linked by the disulfide –S–S– bridges between the Carbon atoms (Fig. 1, b) [20, 21]. However, as was mentioned in Ref. [18] the Cataldo's structures are less probable and have not been proved sufficiently well by spectroscopic data in a contrast to the structure of Woollins (Fig. 1, a).

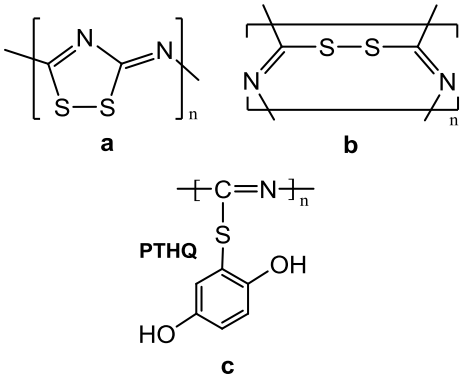

Fig. 1. The different structures of polythiocyanogen $(SCN)_n$ and the proposed structure of synthesized polythiocyanatohydroquinone (PTHQ)

At the same time, we should stress that the S-closed thiocyanates, like the (thiocyanatomethyl)benzene and similar species, [22, 23] would provide predominantly the linear polymerization upon the corresponding conditions. In the present work we have described the first synthesis and spectroscopic IR and UV-vis characterization of the polythiocyanatohydroquinone (hereinafter PTHQ) (Fig. 1,c) together with the DFT assignment of the observed FT-IR and UV-vis spectra.

2. Experimental section

The target PTHQ compound was synthesized by the three-stage synthesis presented in Scheme 1. The 1,4-benzoquinone crystal was dissolved in the glacial acetic acid (GAA) and treated with the NH_4SCN salt in the GGA medium. The forming benzene-1,4-diol and thiocyanogen at the same conditions produce next the *ortho*-substituted 2-thiocyanatobenzene-1,4-diol which polymerizes rapidly into the target PTHQ compound. The orange-brown PTHQ polymer was precipitated by water, filtered, washed and dried upon the 80 °C.

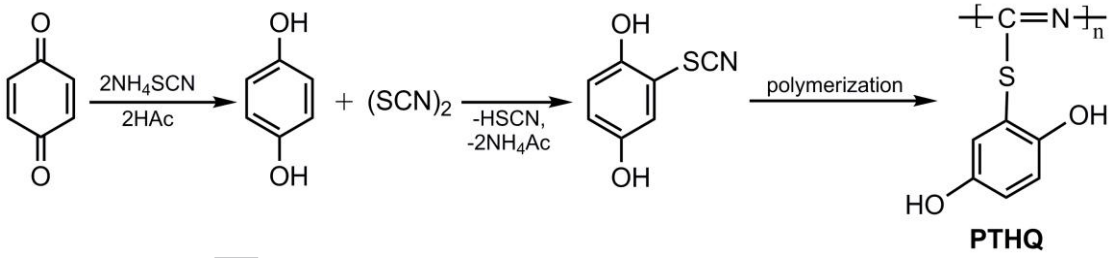

Scheme 1. The three-stage synthesis of polythiocyanatohydroquinone (PTHQ)

The IR spectrum of prepared PTHQ was measured with the PerkinElmer Spectrum One FT-IR Spectrometer in a KBr pellet. The UV-Vis spectrum of the PTHQ has been carried out on a SF-26 spectrophotometer in a DMSO solution with the PTHQ concentration 20 $mg \cdot dm^{-3}$. The transmission electron microscopy (TEM) experiment was carried out using the SELMI TEM 125 K microscope. The XRD pattern analysis was performed by the DRON-3 X-ray diffractometer.

3. Calculation details

The structures of the studied PTHQ oligomeric models (n = 4–8, scheme 1) were optimized by the density functional theory (DFT) method using the B3LYP hybrid functional [24, 25] with the 6-31G(d) basis set. [26] We have also calculated the force fields and IR absorption spectra of the proposed PTHQ models (n = 4–8). All vibrational wavenumbers were found to be real which indicates the finding of the true minimum on the hypersurface of the total

energy of the PTHQ oligomers. In order to compare the calculated IR spectra with the experimental FT-IR data much correctly we have employed the scaling factor equal to 0.980 for the calculated vibrational frequencies in the region 1800–400 cm^{-1}.

The electronic absorption spectra of the studied PTHQ oligomers (n = 4–8) have been calculated by the time-dependent (TD) DFT method [27] with the same B3LYP/6-31G(d) approach using also the polarizable continuum model (PCM) [28] to take into account the solvent effect. We have used the DMSO solvent for the PCM model as well as for the experimental measurements of UV-vis spectrum. The calculated electronic absorption spectra of the PTHQ oligomers were created by using the SWizard software [29] (band half-width 2850 cm^{-1}, Gaussian distribution function). All DFT and TD DTF calculations are performed at the PDC supercomputer of the Royal Institute of Technology (Stockholm) with the usage of the Gaussian09 [30] program package.

4. Results and discussion

4.1. IR spectra of PTHQ

In order to explain the possible structure of the PTHQ compound we have provided the detailed band assignment of the measured IR spectrum (Fig. 2) on the basis of DFT calculations including an additional comparison with the some reference data [31–33].

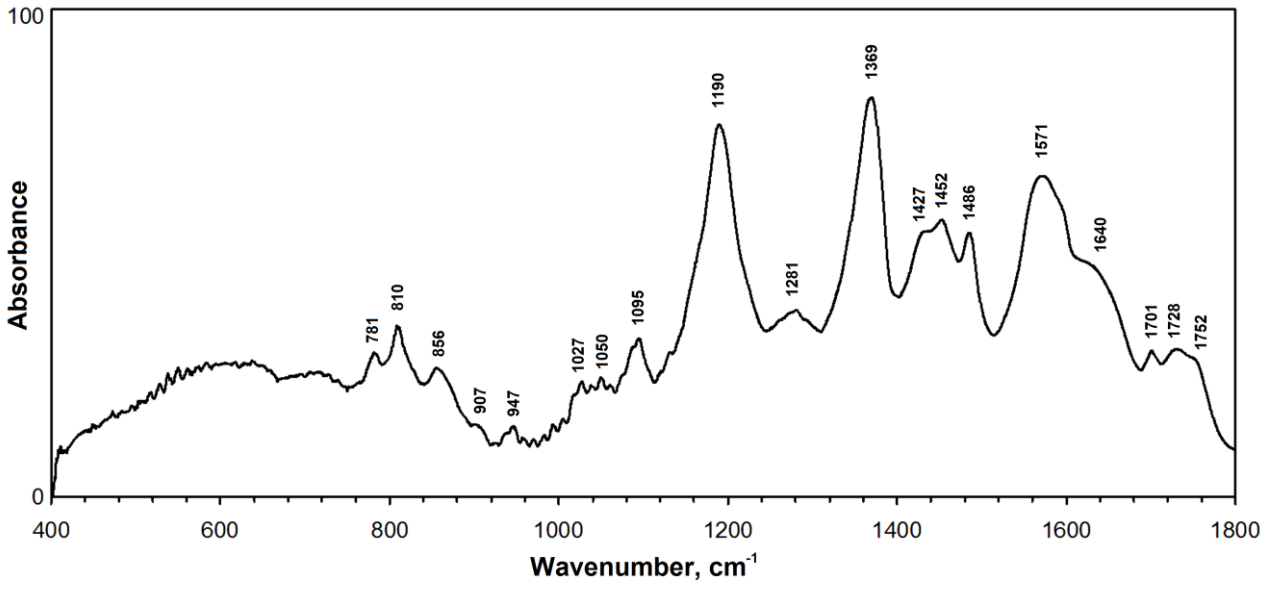

Fig. 2. The experimental IR spectrum of PTHQ polymer measured in KBr pellet.

As one can see from Fig. 2, the measured IR spectrum of PTHQ compound consists of the broad band in the region of 1760–1700 cm^{-1} which can be assigned to the >C=N– stretching vibrations on the basis of our DFT assignment. However, this type of vibrations usually takes place in the region of 1690–1630 cm^{-1} in accordance with the generalized reference data [31]. Such

divergence can be explained by the fact that the PTHQ chains (n = 5–8) consist of almost isolated and very short inner >C=N– bonds (marked by blue color in Fig. 3) with the calculated bond length at about 1.27 Å located between the strongly conjugated CNC fragments. These short >C=N– bonds provide a high-frequency IR absorption above 1700 cm^{-1}. We want to emphasize that the PTHQ chains undergo the breaking due to the steric hindrances for the disposition of 1,4-hydroquinone fragments causing thereby the breach of the conjugated $–(C=N)_n–$ structure and providing therefore the irregular amorphous PTHQ substance. Indeed, for the short (n=4, Fig. 3) and regular $–(C=N)_4–$ chain of the PTHQ polymer the band at about 1740 cm^{-1} is absent in the calculated IR spectrum, but this band appears for the longer $–(C=N)_n–$ chains (n=5–8) in the region of 1750–1720 cm^{-1} in a good agreement with the experimental spectrum (Fig. 2). By this way the synthesized PTHQ compound can be represented as the amorphous mixture of the linear polymeric chains of various length. The amorphous structure of PTHQ polymer has been also clearly seen from the TEM images (Fig. 4) and has additionally confirmed by the absence of any reflections in the XRD pattern spectrum of PTHQ (see supplementary materials**)**.

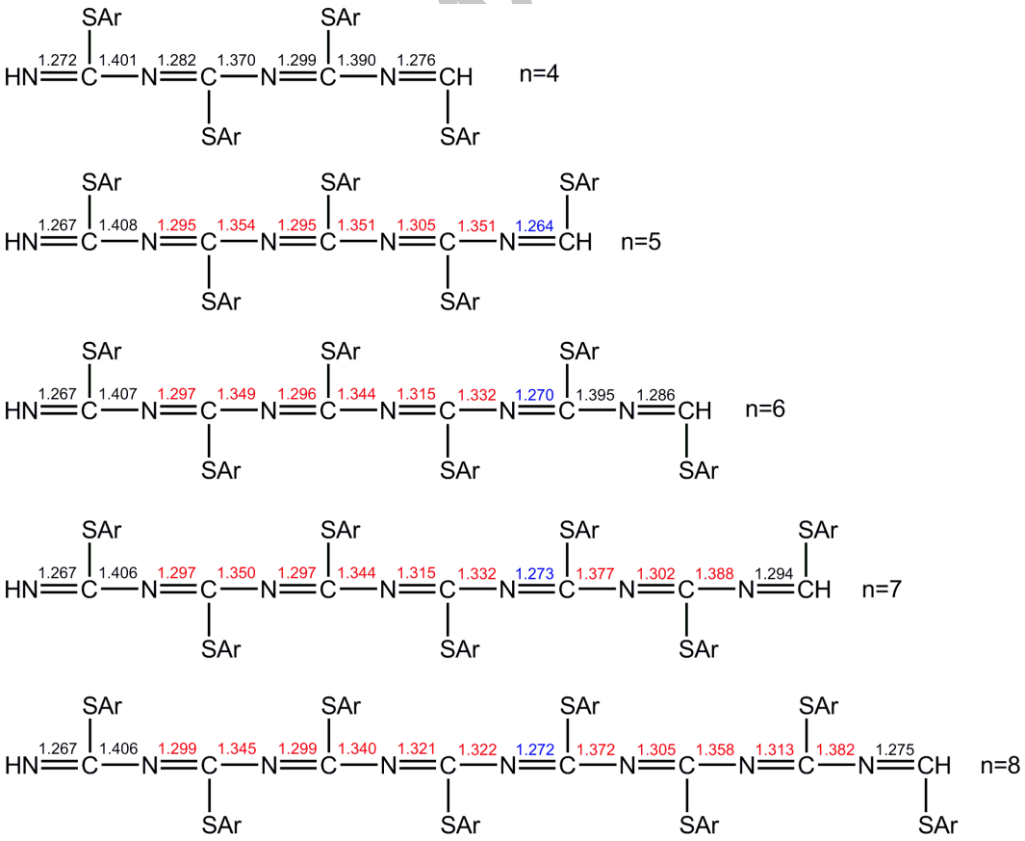

Fig. 3. The Carbon–Nitrogen bond lengths calculated by the B3LYP/6-31G(d) approach for the PTHQ oligomeric $–(C=N)_n–$ chains (n=4–8).

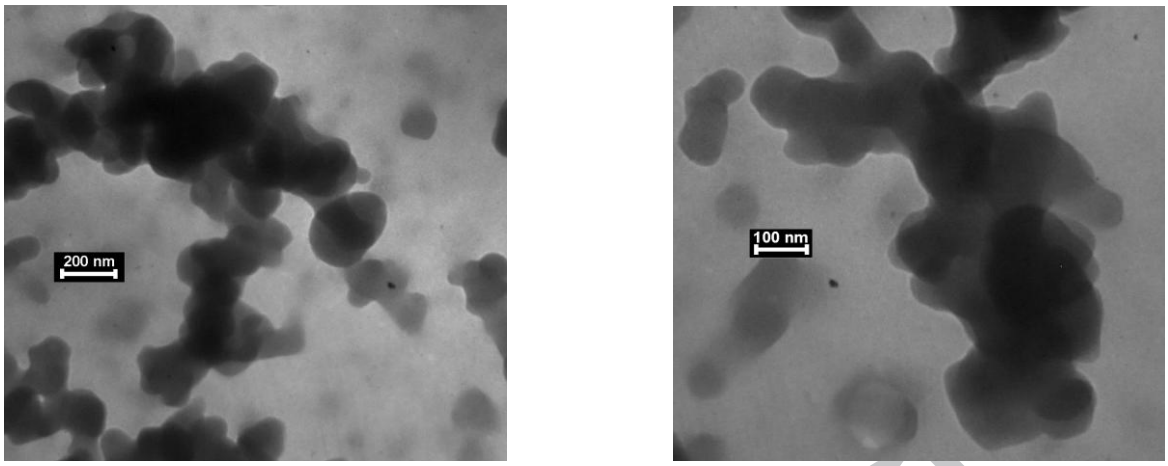

Fig. 4. The TEM images of PTHQ powder measured with the different magnification

The stretching vibrations of the terminal –C=NH and –N=CH bonds and of the inner conjugated –C=N– fragments (marked by red color, Fig. 3) provide in the experimental IR spectrum of PTHQ the strong band with the maximum at 1571 cm^{-1} with the right-side broad shoulder 1700–1615 cm^{-1}. In this region the aromatic C=C stretching vibrations (IR signal at 1640 cm^{-1}) also occurs (calc: 1633 cm^{-1}) in a good agreement with the reference data (the band at about 1660 cm^{-1} usually occurs in the IR spectra of phenols) [31].

The experimental band 1486 cm^{-1} and the neighboring maxima 1452, 1427 cm^{-1} typically correspond to the benzene rings stretching vibrations (Ref. data 1525–1430 [31]); in the calculated oligomers they are mixed with the CNC collective asymmetric stretching vibrations, the CH and OH in-plane bending vibrations (calc.: 1520–1420). The strong broad band with the maximum 1369 cm^{-1} we assigned to the phenolic COH bending vibrations in a good congruence with our DFT calculations (absorption maxima in the region 1370–1307 cm^{-1} for various oligomers; Supplementary materials) and with the reference data for the free benzene-1,4-diol (strong maximum at 1350 cm^{-1}). [32, 33]

The next weak broad band in the detected IR spectrum of PTHQ with the maximum 1281 cm^{-1} corresponds to the C–O stretching vibrations calculated in the region 1307–1225 cm^{-1} together with the CH and OH in-plane bending vibrations. The main OH bending modes also determine the strong absorption band 1190 cm^{-1} clearly observed in IR spectrum of the free benzene-1,4-diol [32, 33]. This band is well reproduced without frequency shift by our DFT calculations for all PTHQ models with the different chain lengths (n=4–8). The well-marked experimental absorption maximum at about 1095 cm^{-1} can be assigned to the –S–Ar stretching vibrations being slightly mixed with the CH in-plane deformations of the benzene-1,4-diol core. [31, 32] The broad absorption region 1070–970 cm^{-1} without clear-cut features in the measured IR spectrum of PTHQ most likely be assigned to the C–S stretching vibrations mixed with the

CH in-plane deformations. [31] In the region of 890–750 cm^{-1} a series of the middle intensity maxima 856, 810, 781 cm^{-1} are observed and should be predominantly assigned to the out-of-plane aromatic CH vibrations. [31–33]

Finally, we wish to point out that the proposed linear structure of the PTHQ compound (Fig. 3) has found a good confirmation from the IR spectral analysis. We have clearly observed and identified the characteristic bands of the >C=N– and –S–Ar moieties, aromatic C=C, CH and phenolic COH groups vibrations which provide a reliable evidence of the proposed structure of the synthesized polymer. In fact, the structure of PTHQ should be much more intricate because the hydroquinone provides upon thiocyanation by the thiocyanogen $(SCN)_2$ reagent not only the mono *ortho*-substituted benzene-1,4-diol species but also the doubly substituted benzene-1,4-diol product occurs. Indeed, we have observed the enhanced Sulfur content in the synthesized PTHQ substance comparing with those for the theoretically predicted linear regular PTHQ chains. Therefore, the real structure of PTHQ can be interpreted as the branched dendrimer-like composition (Scheme 2) which consists of both mono- and doubly- SCN-substituted benzene-1,4-diol moieties.

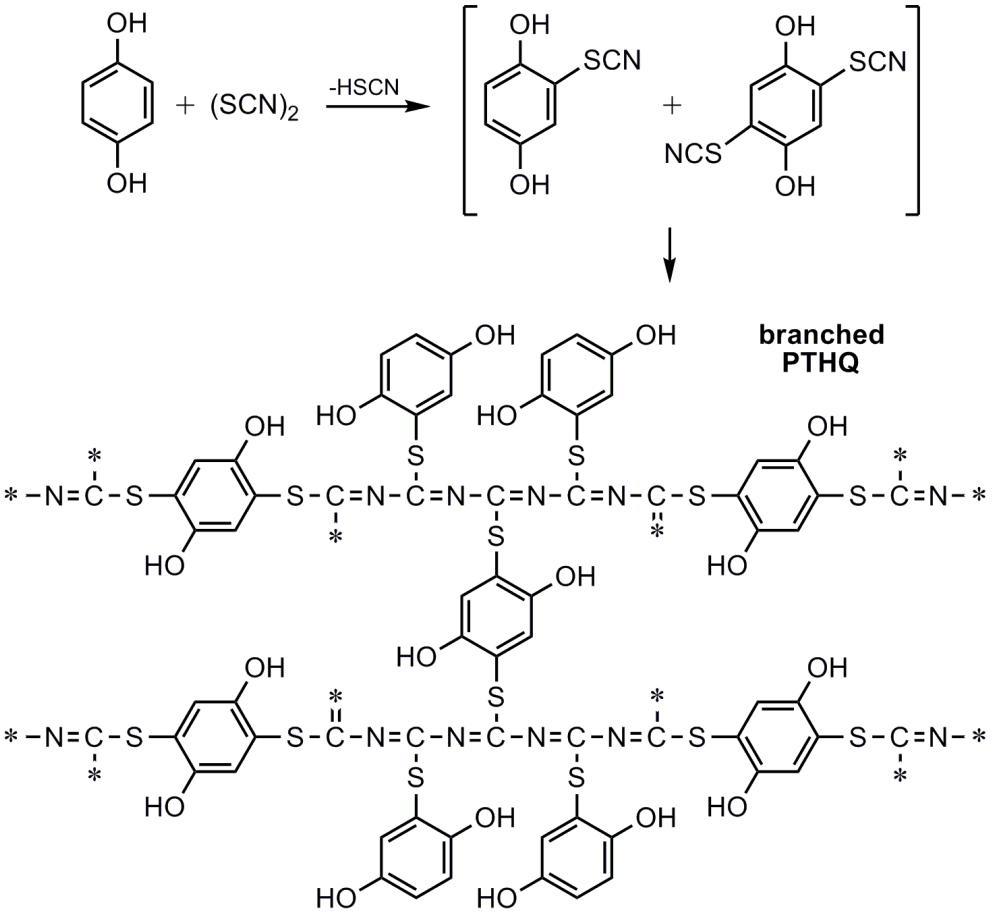

Scheme 2. The synthesis of the branched PTHQ compound through the intermediate mono- and doubly- SCN-substituted benzene-1,4-dioles; (*) denotes the branching points.

4.2. UV-Vis spectra of PTHQ

The synthesized PTHQ powder is almost insoluble in the nonpolar organic solvents, but it demonstrates a good solubility in polar DMSO and aqueous alkaline media. Thus, we have measured the UV-vis spectrum of PTHQ in the DMSO solution in order to prevent deprotonation of the phenolic groups in the aqueous alkaline solution. The experimentally detected UV-vis spectrum of PTHQ is presented in Fig. 5 together with the TD DFT simulated result for the linear PTHQ chain (n=7) which demonstrates the best agreement with experimental spectrum (the calculated spectra for the PTHQ oligomers with n = 4–6, 8 are presented in Supplementary Materials). As one can see from Fig. 5 the experimental UV-vis absorption spectrum of PTHQ consists of the single absorption band with the maximum at 315 nm and of the broad structureless absorption region to the right side. The weak light absorption in the violet-blue region provides the light yellow color of the studied PTHQ solution. It is also possible to note separately the weak shoulder at about 360 nm in the experimental spectrum (fig. 5, curve 1).

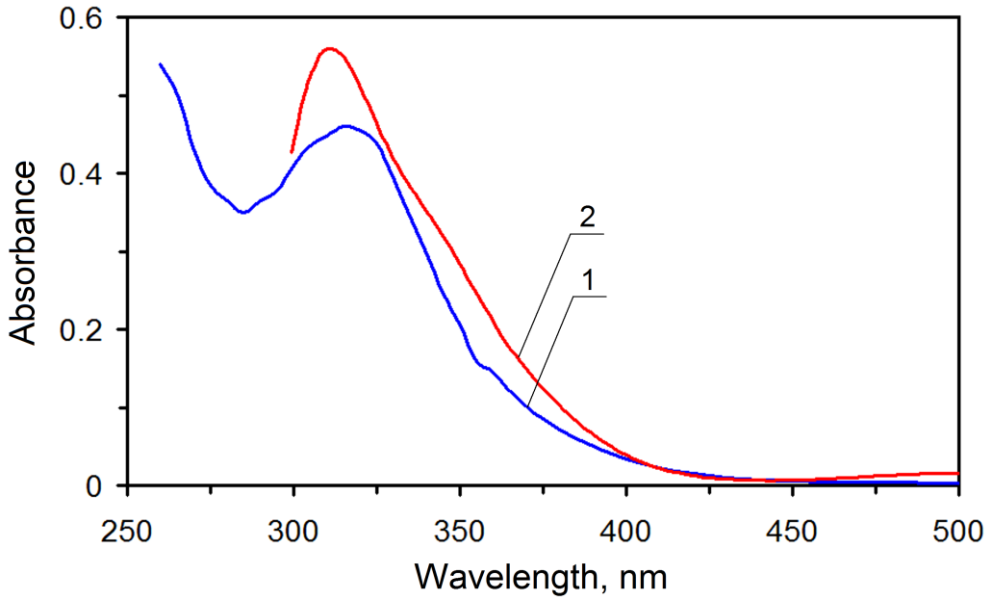

Fig. 5. UV-vis absorption spectrum of PTHQ in DMSO solution (blue curve 1) in comparison with the TD DFT/B3LYP/6-31G(d) calculated spectrum (red curve 2) for the PTHQ chain (n = 7) (account of the solvent by the PCM model is also applied).

The measured UV-vis absorption spectrum of PTHQ is well reproduced by our TD DFT/B3LYP/6-31G(d) calculation (Fig. 5, curve 2) for the PTHQ oligomer with n=7. The experimental strong maximum at 315 nm corresponds to a number of high-lying singlet exited states (S_{20}–S_{35}) in the region 300–330 nm (Table 1 for n = 7; for the n = 4–6, 8 see Supplementary Materials).

Table. 1. Wavelengths (λ), oscillator strengths (f) and orbital assignment of the selected electronic transitions in the calculated absorption spectrum of the PTHQ oligomer (n=7).

State	λ, nm	f	Assignment
S_1 ($\pi\pi^*$)	551	0.0116	HOMO → LUMO (99%)
S_3 ($\pi\pi^*$)	498	0.0141	HOMO-4 → LUMO (99%)
S_{15} ($\pi\pi^*$)	371	0.0923	HOMO-9 → LUMO (59%) HOMO-7 → LUMO (27%)
S_{17} ($\pi\pi^*$)	351	0.0419	HOMO-8 → LUMO (74%)
S_{18} ($\pi\pi^*$)	343	0.2332	HOMO-11 → LUMO (89%)
S_{21} ($\pi\pi^*$)	321	0.0732	HOMO-10 → LUMO (59%) HOMO-7 → LUMO+1 (25%)
S_{22} ($\pi\pi^*$)	320	0.1705	HOMO-7 → LUMO+1(49%) HOMO-10 → LUMO (24%)
S_{30} ($\pi\pi^*$)	305	0.1437	HOMO-20 → LUMO (31%) HOMO-19 → LUMO (15%)

Theoretically predicted broad shoulder in the region of 330–500 nm corresponds mainly to the $S_0 \rightarrow S_{18}$, $S_0 \rightarrow S_{17}$ and $S_0 \rightarrow S_{15}$ vertical electronic transitions calculated at the 343, 351 and 371 nm, respectively. Thus, the shape of the simulated curve 2 in the region 330–500 nm agrees well with the experimental curve 1 (Fig. 5) except the calculated very weak absorption at the long wavelengths (the low-lying states S_3 and S_1 in Table 1); in the experiment such weak absorption is detected at the noise level. As follows from the analysis of molecular orbitals isosurfaces (Fig. 6) all these states presented in Table 1 correspond to the $\pi\pi^*$ type excitations of the charge transfer nature. It can be seen from Fig. 6 that the electron density of all occupied MOs undergoes a strong shift upon the electronic excitation from the hydroquinone moieties to the $-(C=N)_3-$ conjugated fragment at the end of oligomer chain (LUMO, Fig. 6). Here we present the low-lying occupied orbitals since they are responsible for the most intense UV absorption bands.

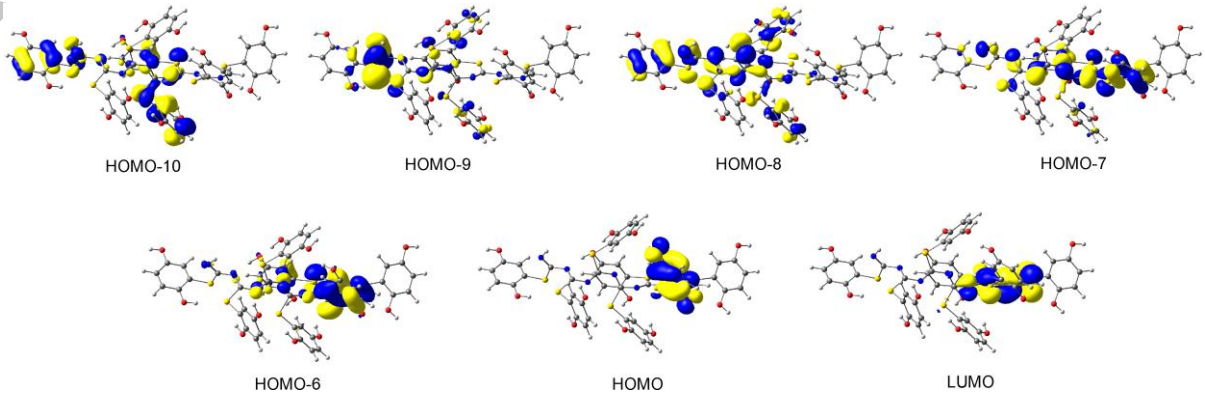

Fig. 6. The shape of selected molecular orbitals of the PTHQ oligomer (n=7) (controlling value of the isosurface is 0.03 a.u.).

The orbital nature of the electronic transitions in the absorption spectra of the other PTHQ oligomers (n = 4–6, 8) is quite similar and also corresponds to the charge-transfer configurations. The only difference concerns the number of quasidegenerate electronic states which correspond to the charge transfer transitions from the number of hydroquinone moieties (n = 4–6, 8) to the common nature LUMO or LUMO+1 orbitals. The pendant mono- and doubly-SCN-substituted benzene-1,4-diol moieties do not provide large differences in calculated spectra and in the orbital nature of the excited states. In comparison with the typical conjugated polymers [3, 4, 34] the synthesized PTHQ is a partly conjugated compound with numerous breaches in the π-extended chain. Thus, the low-lying excited states (HOMO→LUMO excitation, Fig. 5) are localized on the hydroquinone moiety with a charge transfer to the part of the chain. Therefore, we can not anticipate the exciton behavior [34], photo-conductivity and semiconducting properties of the synthesized PTHQ polymer.

5. Conclusions

In the present work we have developed the first protocol for the synthesis of polythiocyanatohydroquinone compound. The proposed synthesis procedure is very simple and includes only three stages occurring without catalyst and initiator of polymerization under the normal conditions. The obtained polymer has been comprehensively studied with the FT-IR, UV-vis spectroscopic methods, by the XRD pattern analysis and TEM technique. Our computational results support a branched polymeric structure of the PTHQ compound which is composed from the linear fragments of different length. The branched structure of PTHQ can be principally explained by the stochastic copolymerization of both mono- and doubly- SCN-substituted benzene-1,4-diol moieties. The synthesized PTHQ material demonstrates a good ability to stabilize the colloidal solutions of the noble metals nanoparticles; this PTHQ peculiarity is useful for the long-term storage and size-controlling of such colloids. [35–37] In this connection the novel metal-containing composite materials are planned to be synthesized in near future from such precipitated colloids by pyrolysis in inert atmosphere.

6. Acknowledgments

All computations are performed with the help of resources provided by the Swedish National Infrastructure for Computing (SNIC) at the Parallel Computer Center (PDC) through the project ‘Multiphysics Modeling of Molecular Materials’, SNIC 020/11-23. This research was also supported by the Ministry of Education and Science of Ukraine (project number 0113U001694).

7. Appendix A. Supplementary material

Supplementary data associated with this article can be found, in the online version, at http://10.1016/j.molstruc.XXXX.XX.XXX.

Reference

[1] A. Facchetti, Chem. Mater. 23 (2011) 733–758.

[2] X. Guo, M. Baumgarten, K. Müllen, Prog. Polym. Sci. 38 (2013) 1832–1908.

[3] B. Minaev, G. Baryshnikov, H. Agren, Phys. Chem. Chem. Phys. 16 (2014) 1719–1758.

[4] M. Grigoras, A.M. Catargiu, T. Ivan, L. Vacareanu, B. Minaev, E. Stromylo, Dyes Pigm. 113 (2015) 227–238.

[5] R. Gutzler, D. F. Perepichka, J. Am. Chem. Soc. 135 (2013) 16585–16594.

[6] F. Schlütter, T. Nishiuchi, V. Enkelmann, K. Müllen, Angew. Chem. Int. Ed. 53 (2014) 1538–1542.

[7] N.N. Karaush, G.V. Baryshnikov, B.F. Minaev, Chem. Phys. Lett. 612 (2014) 229–233.

[8] L. Lafferentz, V. Eberhardt, C. Dri, C. Africh, G. Comelli, F. Esch, S. Hecht, L. Grill, Nat. Chem. 4 (2012) 215–220.

[9] E.L. Spitler, W.R. Dichtel, Nat. Chem. 2 (2010) 672–677.

[10] G.V. Baryshnikov, B.F. Minaev, N.N. Karaush, V.A. Minaeva, RSC Adv. 4 (2014) 25843–25851.

[11] E. Söderbäck, Justus Liebigs Ann. Chem. 419 (1919) 217–321.

[12] Z. Toth, M. Okros, M.T. Beck, Inorg. Chim. Acta. 143 (1988) 9–11.

[13] Z. Toth, Z. Zsoter, M.T. Beck, React. Kinet. Catal. Lett. 47 (1992) 29–35.

[14] Z. Toth, P. Penzeli, E. Posan, React. Kinet. Catal. Lett. 56 (1995) 185–190.

[15] M.-H. Kim, J.M. Kim, Y.-U. Kwon, Solid State Phenom. 119 (2007) 13–16.

[16] P. Krishnan, S. G. Advani, A. K. Prasad, J. Power Sources. 196 (2011) 7755–7759.

[17] V.P.S. Perera, P.V.V. Jayaweera, P.K.D.D.P. Pitigala, P.K.M. Bandaranayake, G. Hastings, A.G.U. Perera, K. Tennakone, Synth. Metals. 143 (2004) 283–287.

[18] W.R. Bowman, C.J. Burchell, P. Kilian, A.M.Z. Slawin, P. Wormald, J.D. Woollins, Chem. Eur. J. 12 (2006) 6366–6381.

[19] F. Cataldo, Polyhedron 11 (1992) 79–83.

[20] F. Cataldo, J. Inorg. Organomet. Polym. 7 (1997) 35–50.

[21] F. Cataldo, Y. Keheyan, Polyhedron 21 (2002) 1825–1835.

[22] A.W. Erian, S.M. Sherif, Tetrahedron 55 (1999) 7957–8024.

[23] M.A.K. Zarchi, J. Chinese Chem. Soc. 54 (2007) 1299–1302.

[24] A.D. Becke, J. Chem. Phys. 98 (1993) 5648–5652.

[25] C. Lee, W. Yang, R.G. Parr, Phys. Rev. B 37 (1988) 785–789.

[26] M.M. Francl, W.J. Pietro, W.J. Hehre, J.S. Binkley, D.J. DeFrees, J.A. Pople, M.S. Gordon, J. Chem. Phys. 77 (1982) 3654–3665.

[27] E. Runge, E. K. U. Gross, Phys. Rev. Lett. 52 (1984) 997–1000.

[28] S. Miertuš, E. Scrocco, J. Tomasi, Chem. Phys. 55 (1981) 117–129

[29] S.I. Gorelsky, SWizard program, http://www.sg-chem.net, University of Ottawa, Ottawa, Canada, 2013

[30] M. J. Frisch, G. W. Trucks, H. B. Schlegel, G. E. Scuseria, M. A. Robb, J. R. Cheeseman, G. Scalmani, V. Barone, B. Mennucci, G. A. Petersson, H. Nakatsuji, M. Caricato, X. Li, H. P. Hratchian, A. F. Izmaylov, J. Bloino, G. Zheng, J. L. Sonnenberg, M. Hada, M. Ehara, K. Toyota, R. Fukuda, J. Hasegawa, M. Ishida, T. Nakajima, Y. Honda, O. Kitao, H. Nakai, T. Vreven, J. A. Montgomery, Jr., J. E. Peralta, F. Ogliaro, M. Bearpark, J. J. Heyd, E. Brothers, K. N. Kudin, V. N. Staroverov, R. Kobayashi, J. Normand, K. Raghavachari, A. Rendell, J. C. Burant, S. S. Iyengar, J. Tomasi, M. Cossi, N. Rega, J. M. Millam, M. Klene, J. E. Knox, J. B. Cross, V. Bakken, C. Adamo, J. Jaramillo, R. Gomperts, R. E. Stratmann, O. Yazyev, A. J. Austin, R. Cammi, C. Pomelli, J. W. Ochterski, R. L. Martin, K. Morokuma, V. G. Zakrzewski, G. A. Voth, P. Salvador, J. J. Dannenberg, S. Dapprich, A. D. Daniels, O. Farkas, J. B. Foresman, J. V. Ortiz, J. Cioslowski, D. J. Fox, Gaussian, Inc., Wallingford CT, Gaussian 09. Rev. A.02 (2009).

[31] G. Socrates, Infrared and Raman characteristic group frequencies: tables and charts, John Wiley & Sons Ltd., 2001.

[32] M.J. Kubinyi, G. Keresztury, Mikrochim. Acta Suppl., 14 (1997) 525–528.

[33] Coblentz Society, Inc., "Evaluated Infrared Reference Spectra" in NIST Chemistry WebBook, NIST Standard Reference Database Number 69, Eds. P.J. Linstrom, W.G. Mallard, National Institute of Standards and Technology, Gaithersburg MD, 20899, http://webbook.nist.gov.

[34] L. L. G. Justino, M. L. Ramos, P. E. Abreu, A. Charas, J. Morgado, U. Scherf, B. F. Minaev, H. Ågren, H. D. Burrows, J. Phys. Chem. C 117 (2013) 17969–17982.

[35] V.A. Litvin, R.L. Galagan, B.F. Minaev, Colloids Surf. A, 441 (2012) 234–243

[36] V.A. Litvin, B.F. Minaev, Spectrochim. Acta A 108 (2013) 115–122.

[37] V.A. Litvin, B.F. Minaev, Mater. Chem. Phys. 144 (2014) 168–178.

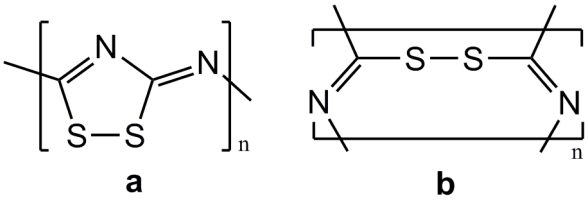

a b

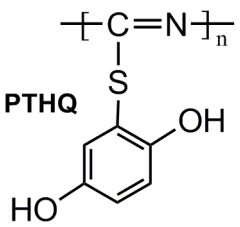

c

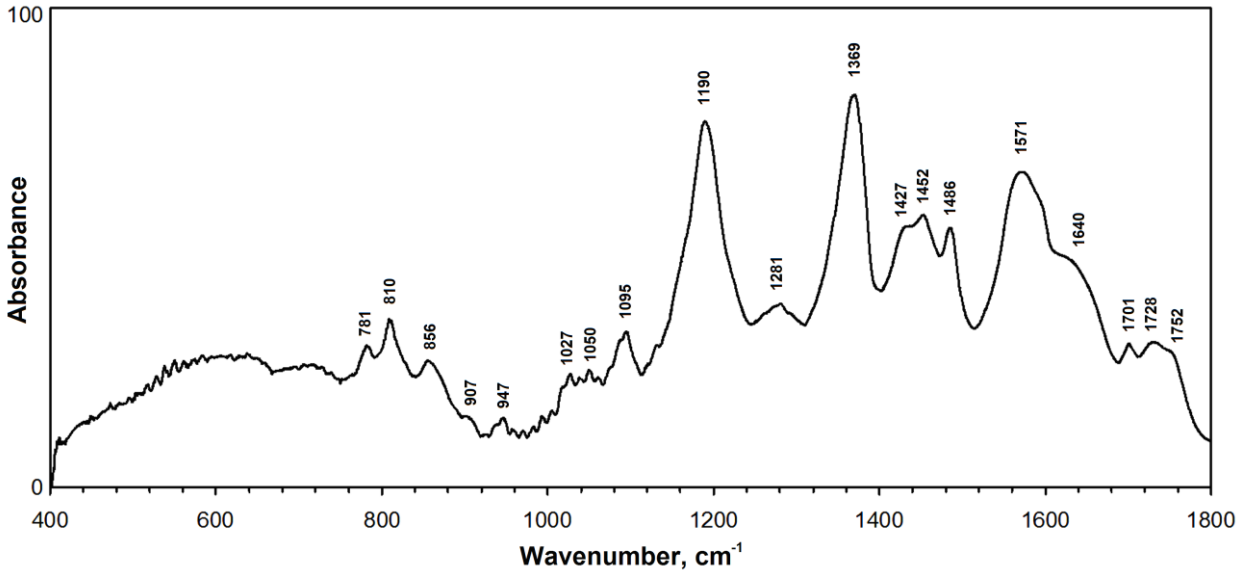

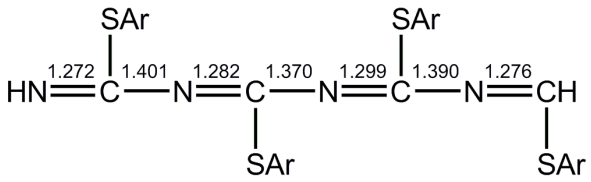
SAr
SAr
1.272
1.401
1.282
1.370
1.299
1.390
1.276
HN
C
N
C
N
C
N
CH
SAr
SAr

n=4

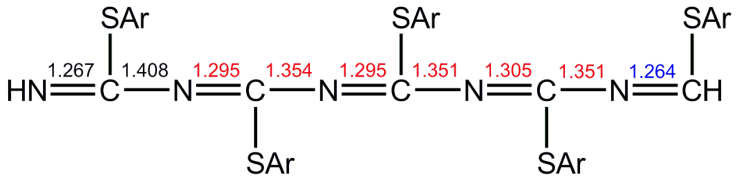
SAr
SAr
SAr
1.267
1.408
1.295
1.354
1.295
1.351
1.305
1.351
1.264
HN
C
N
C
N
C
N
C
N
CH
SAr
SAr

n=5

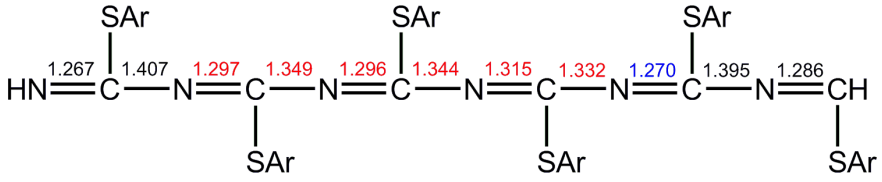
SAr
SAr
SAr
1.267
1.407
1.297
1.349
1.296
1.344
1.315
1.332
1.270
1.395
1.286
HN
C
N
C
N
C
N
C
N
C
N
CH
SAr
SAr
SAr

n=6

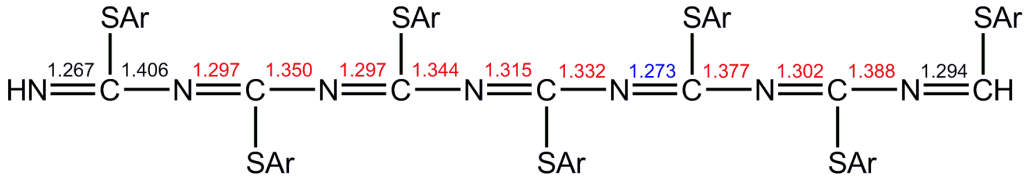
SAr
SAr
SAr
SAr
1.267
1.406
1.297
1.350
1.297
1.344
1.315
1.332
1.273
1.377
1.302
1.388
1.294
HN
C
N
C
N
C
N
C
N
C
N
C
N
CH
SAr
SAr
SAr

n=7

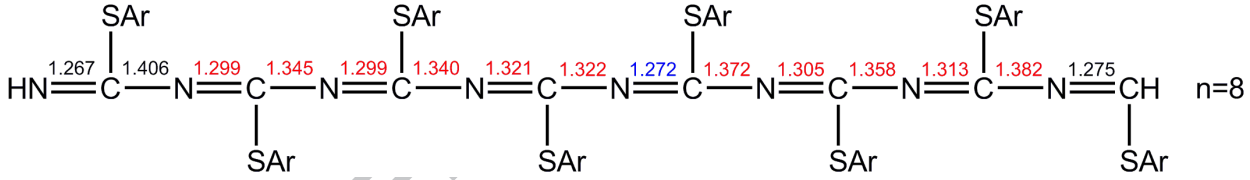
SAr
SAr
SAr
SAr
1.267
1.406
1.299
1.345
1.299
1.340
1.321
1.322
1.272
1.372
1.305
1.358
1.313
1.382
1.275
HN
C
N
C
N
C
N
C
N
C
N
C
N
C
N
CH
SAr
SAr
SAr

n=8

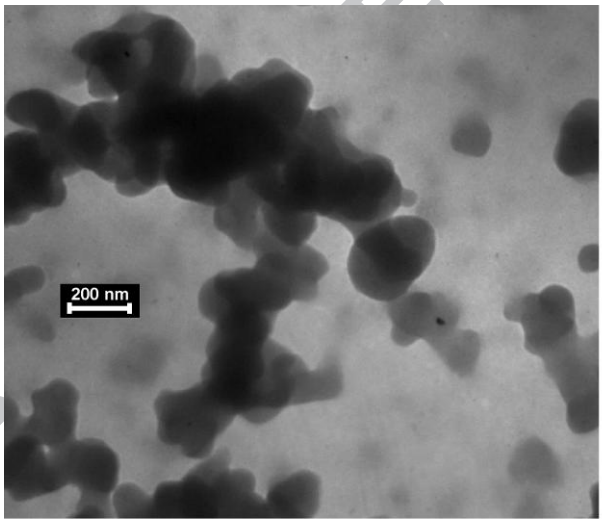
200 nm

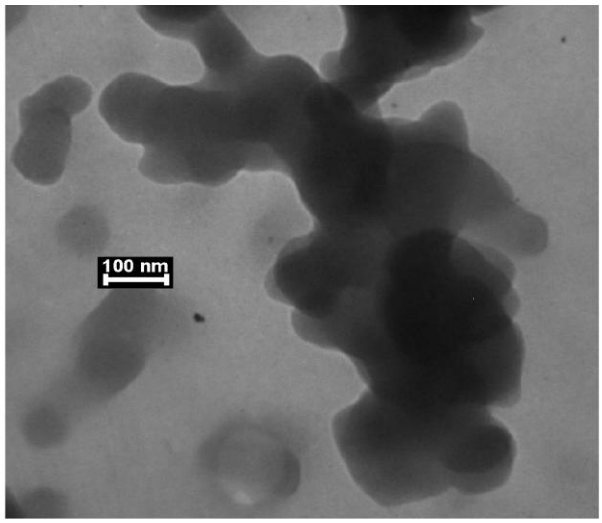
100 nm

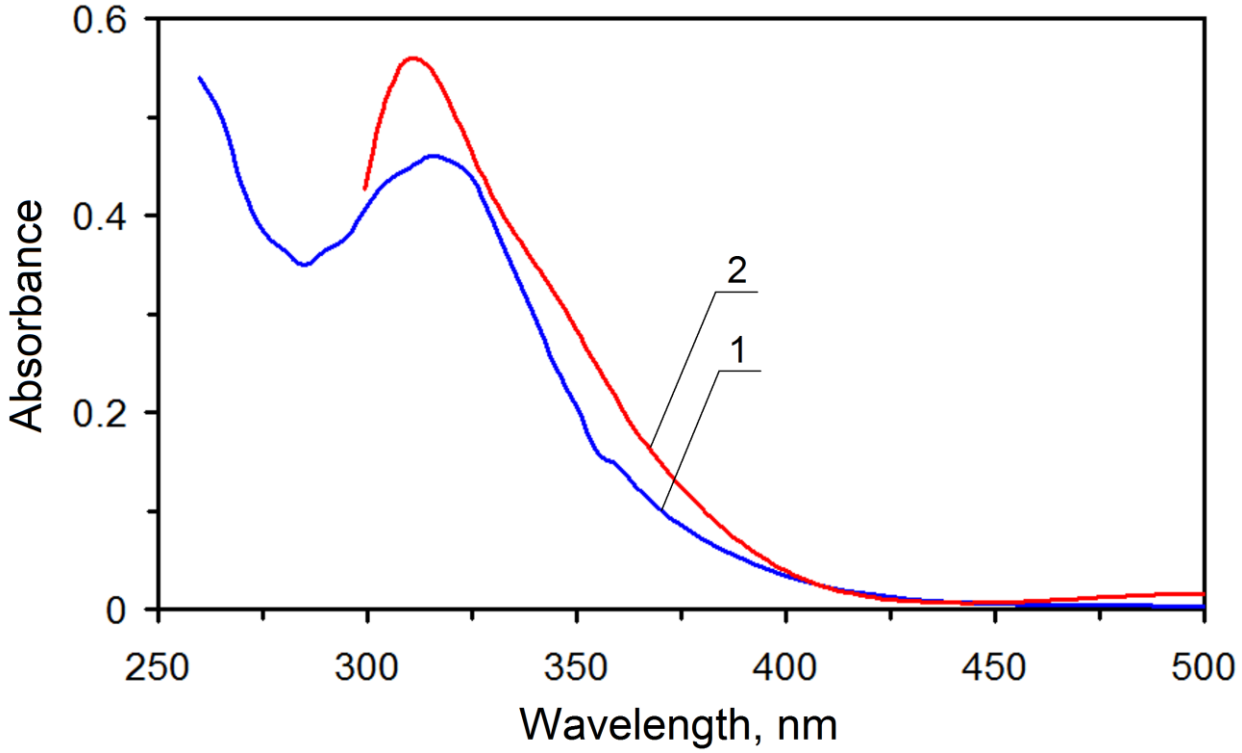
0.6
0.4
0.2
0
Absorbance
2
1
250
300
350
400
450
500
Wavelength, nm

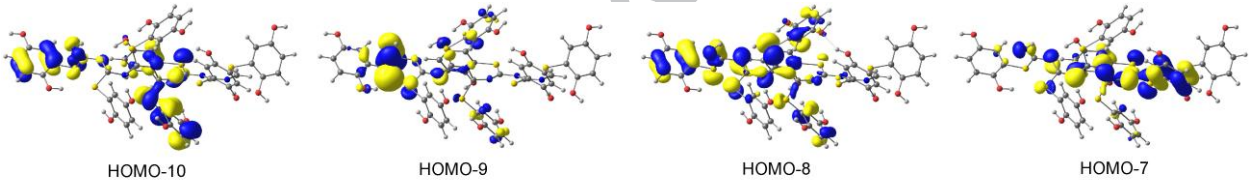
HOMO-10
HOMO-9
HOMO-8
HOMO-7

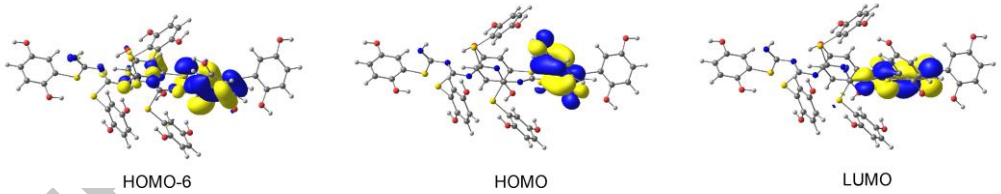
HOMO-6
HOMO
LUMO

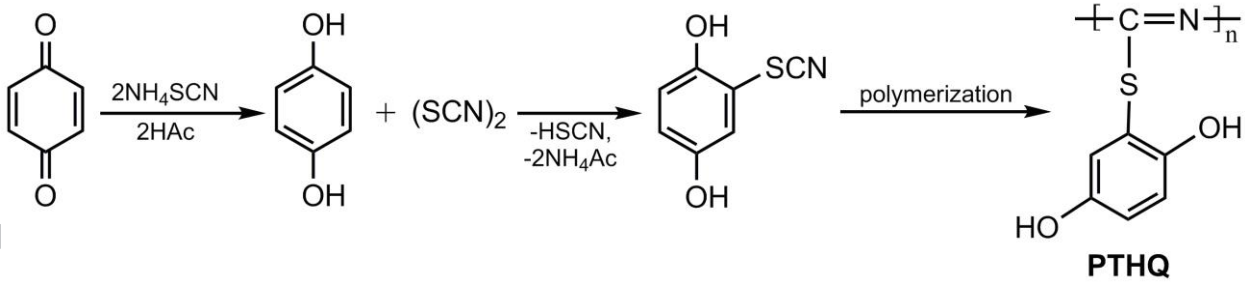
O
O
2NH4SCN
2HAc
OH
OH
+ (SCN)2
-HSCN,
-2NH4Ac
OH
SCN
OH
polymerization
C=N
n
S
OH
HO
PTHQ

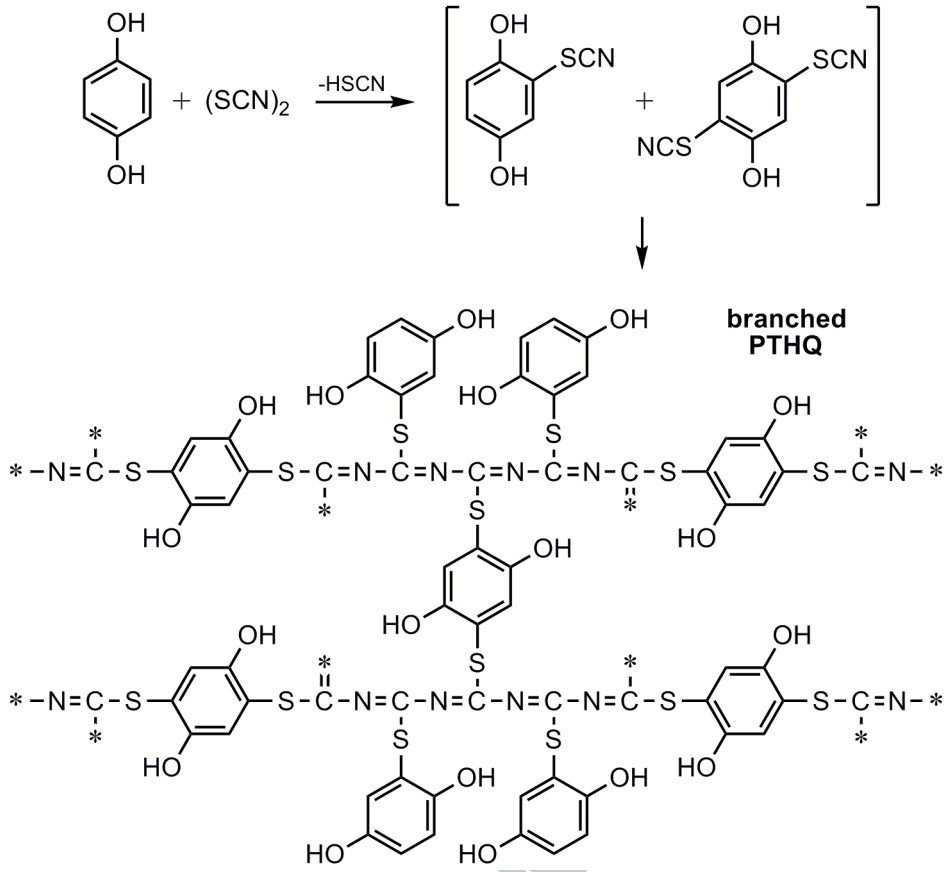

Graphical abstract

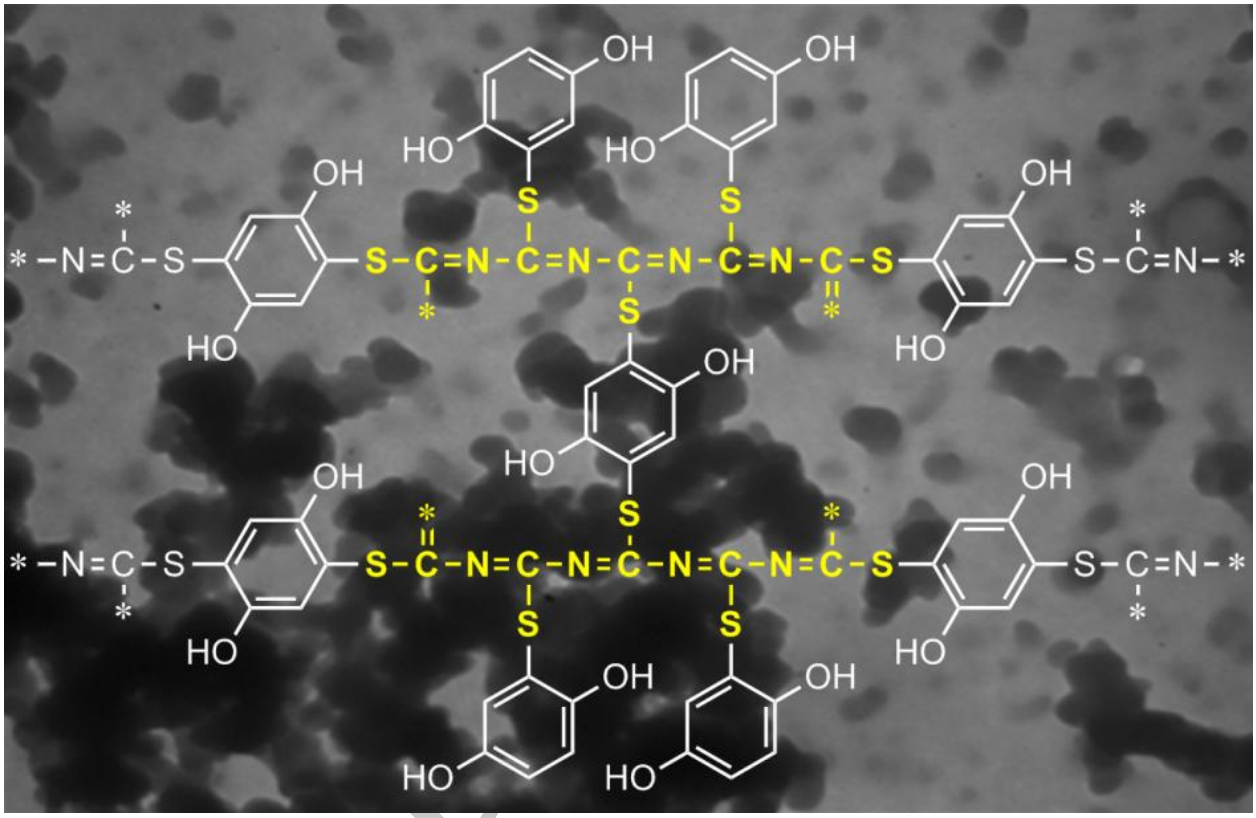

Highlights

- The branched polymer was synthesized from the 1,4-benzoquinone and NH_4SCN reagents.
- The polymer represents $(aryl\text{-}SCN)_n$ compound named polythiocyanatohydroquinone.
- DFT calculations confirm the linear chain structure of polymer.
- XRD pattern analysis indicates the amorphous structure of the synthesized polymer.
- This new material stabilizes the colloidal solutions of Ag and Au nanoparticles**.**